Raman scattering from triple perovskites with the $Ba_2YCu_3O_x$ structure: Normal mode assignments from substitutions on the Ba site

Michael Stavola, D. M. Krol, L. F. Schneemeyer, S. A. Sunshine, J. V. Waszczak, and S. G. Kosinski
AT&T Bell Laboratories, Murray Hill, New Jersey 07974
(Received 25 July 1988)

Raman spectra are reported for $Ba_{1.5}La_{1.5}Cu_3O_{7+\delta}$ ceramics and $Sr_2YCu_{3-x}Al_xO_{7-\delta}$ ceramics and single crystals. The shifts in the frequencies of the Raman features for these triple perovskites, as compared to $Ba_2YCu_3O_x$, provide additional evidence for the assignments of the normal modes. There are large changes in the frequency of the prominent 500-cm^{-1} feature that are well correlated to changes in the lengths of the axial Cu—O bonds. This correlation supports the assignment of the 500-cm^{-1} feature to the axial stretching of the oxygen atoms that bridge the Cu sites. The substitution of Sr for Ba does not change the frequency of the 140-cm^{-1} mode of $Ba_2YCu_3O_x$, thereby supporting its assignment to axial stretching of the planar Cu atoms rather than to a Ba mode. With these new data and the previous, definitive assignment of the feature at 340 cm^{-1}, the assignments of the five prominent Raman modes are well supported by experiment and agree with lattice-dynamics calculations.

I. INTRODUCTION

Since the discovery of high-temperature superconductivity in $Ba_2YCu_3O_7$, several groups have reported Raman spectra of this and related materials.[1-13] In spite of dozens of studies, the assignment of the vibrational normal modes remains controversial. The phonons, in addition to their possible role in the mechanism of superconductivity,[14] show an interesting dependence of frequency upon temperature[1,5,13] and coupling to electronic states;[15] the interpretation of these effects and also material characterization by Raman techniques depend critically on the phonon assignments. Here, we report results on compounds with the $Ba_2YCu_3O_x$ triple perovskite structure that have been substituted on the Ba site. The resultant changes in the vibrational frequencies provide additional evidence for the assignments of the vibrational modes.

The unit cell[16] (space group *Pmmm*) of $Ba_2YCu_3O_7$ is shown in Fig. 1, for reference, with the atoms labeled according to the notation of Siegrist *et al.*[17] The atoms of the square-planar cuprate layers are labeled Cu(2), O(2), and O(3). The chain atoms are labeled Cu(1) and O(4). The O(1) atoms bridge the Cu(2) and Cu(1) layers. A factor group analysis of the $Ba_2YCu_3O_7$ structure shows that there are 15 Raman active modes with 5 of A_g, 5 of B_{2g}, and 5 of B_{3g} symmetry (in the point group D_{2h}). In practice, only the 5 A_g modes are observed.

Raman features have been observed near 500, 435, 340, 140, and 116 cm^{-1} for $Ba_2YCu_3O_7$ in studies of single crystals.[7-13] Weak, sample-dependent features have also been observed near 600 and 220 $cm.^{-1}$ Studies of the polarization characteristics of the Raman scattering from single crystals coupled with calculations of the lattice dynamics[2,11,18] have provided the most convincing assignments of these features. However, definitive assignments cannot be made on the basis of the polarization measurements because all of these vibrations have polarization selection rules consistent with A_g modes for the D_{2h} point group. Only the 335-cm^{-1} mode can be assigned with certainty because it shows selection rules characteristic of a B_{1g} mode for the tetragonal D_{4h} point group (the orthorhombic distortion is small) and just one normal mode has this symmetry.[11]

Here, we report spectra for two types of materials with the triple perovskite structure, both semiconducting, that have been substituted on the alkaline earth site. One type of sample is $Ba_{1.5}La_{1.5}Cu_3O_{7+\delta}$ which is an end member of the solid solution $Ba_{2-x}La_{1+x}Cu_3O_{7+\delta}$ (Refs. 19 and 20) and has a partial substitution of Ba by La. Another set of samples contain Sr in place of Ba. While the solid solution $(Ba,Sr)_2YCu_3O_{7-\delta}$ extends only to $Ba_{1.2}Sr_{0.8}YCu_3O_{7-\delta}$ the partial substitution of Cu(1) atoms by Al stabilizes the perovskite structure for complete Ba re-

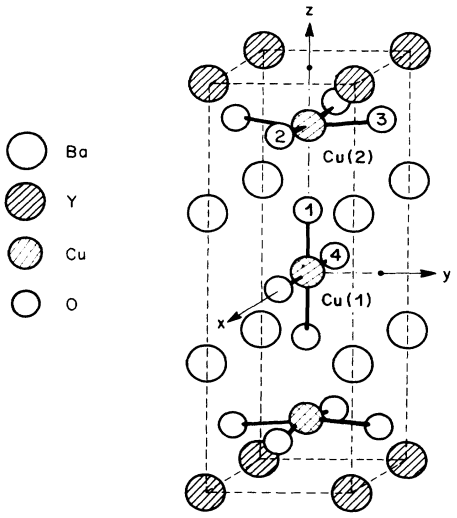

FIG. 1. A unit cell of $Ba_2YCu_3O_7$ [after L. F. Mattheis and D. R. Hamann, Solid State Commun. **63**, 395 (1987)]. Oxygen atoms are labeled according to the notation of Siegrist *et al.*, Ref. 17.

placement by Sr in $Sr_2YCu_{3-x}Al_xO_{7-\delta}$ (Ref. 21). These substitutions cause large changes in the Cu(1)—O(1) and Cu(2)—O(1) bond lengths and the oxygen-related vibrational frequencies with respect to those of $Ba_2YCu_3O_x$. The correlation of frequency with bond length provides support for the assignment of the 500 cm^{-1} feature to O(1) axial stretching.[22] The change in the low-frequency features upon substitution of Sr for Ba provides new evidence for the assignment of the 140 cm^{-1} feature to the mode associated with axial Cu(2) stretching.

II. EXPERIMENTAL PROCEDURE

Ceramic pellets of $Ba_{1.5}La_{1.5}Cu_3O_{7.25}$ and $Sr_2YCu_{3-x}Al_xO_{7-\delta}$ were made by standard techniques with repeated grindings and firings (usually three or four). For the Sr compound, single-phase samples were obtained for Al contents of $0.4 \leq x \leq 0.9$. Samples were given a final anneal in 1 atm of O_2 at 500 °C to maximize oxygen content. Oxygen content was determined by hydrogen reduction in a thermogravimetric analysis (TGA) apparatus. For the $Sr_2YCu_{3-x}Al_xO_{7-\delta}$ ceramics, it was determined that $\delta \approx 0$. Furthermore, oxygen does not readily evolve from these samples, even when annealed in N_2 at temperatures near 700 °C (Ref. 21).

Single crystals of $Sr_2YCu_{3-x}Al_xO_{7-\delta}$ were grown from Cu-O-rich melts contained in alumina crucibles.[21] Aluminum from the crucible contaminates the melt and stabilizes the perovskite phase. The structure of such crystals has been examined by x-ray diffraction. From the occupation parameter refinements it was determined that Al substitution was confined to the Cu(1) site (similar to what has been observed for Al substitution in $Ba_2YCu_3O_x$) with a typical ratio of Cu(1) to Al of 1 to 2, i.e., a composition of $Sr_2YCu_{2.33}Al_{0.67}O_{7-\delta}$. Crystals were either annealed in oxygen for 7 days near 450 °C or annealed in N_2 for 20 h at 700 °C. The Raman spectra were not sensitive to these annealing treatments (consistent with the near constancy of oxygen content observed for ceramics).

The crystals were square platelets with areas of a few mm^2 and a thickness of a few tenths of a mm with the c axis normal to the basal plane. The crystallographic axes are along the crystal edges. For crystals with orthorhombic symmetry, a and b were not distinguished because of microtwinning.

Raman measurements were made at room temperature with an ISA double spectrometer equipped with photon counting detection. The system includes a Raman microscope which was used to record backscattering spectra from the thin crystal edges. For ceramics and the c face of crystals, spectra were measured in a 90° scattering geometry. The spectrometer resolution was 5 cm^{-1} in all cases. The 5145 or 4880-Å lines of an Ar ion laser were used for excitation with an incident power of ≤ 4 mW in the microscope and of ≤ 100 mW for the 90° scattering experiments. For the low-frequency range, $\omega \lesssim 200$ cm^{-1}, the samples were measured while in an Ar atmosphere to eliminate the Raman features from air.

In the backscattering measurements, the incident and scattered light have their propagation vectors along the x direction [parallel to the a (or b) axis] with electric vectors along y or z where z is along the c axis.

In the 90° scattering measurements, the c axis is in the scattering plane. For the xx geometry the x and y axes are parallel to the crystallographic axes and the incident and scattered light have their electric vectors along x. For the xy geometry, the incident and scattered light have their electric vectors along x and y, respectively. For the geometries labeled $x'x'$ and $x'y'$ the crystal has been rotated by 45° about the c axis so that x' and y' are $\pm 45°$ from the a axis of the crystal.

III. RESULTS AND DISCUSSION

The A_g vibrations of the $Ba_2YCu_3O_x$ structure involve the following atomic motions along the c axis: (i) axial motion of the O(1) atoms, (ii) Cu(2)—O(2) and Cu(2)—O(3) bond bending with the O(2) and O(3) atoms moving in phase, (iii) Cu(2)—O(2) and Cu(2)—O(3) bond bending with the O(2) and O(3) atoms moving out of phase, (iv) axial stretching of the Cu(2) atoms, and (v) axial stretching of the Ba atoms.

These modes are illustrated in Fig. 2. The orthorhombic distortion is small in $Ba_2YCu_3O_7$ and even smaller in the Sr compound (see Table I). For tetragonal symmetry, point group D_{4h}, the motions (i), (ii), (iv), and (v) correspond to the A_{1g} modes and motion (iii) to the B_{1g} mode.

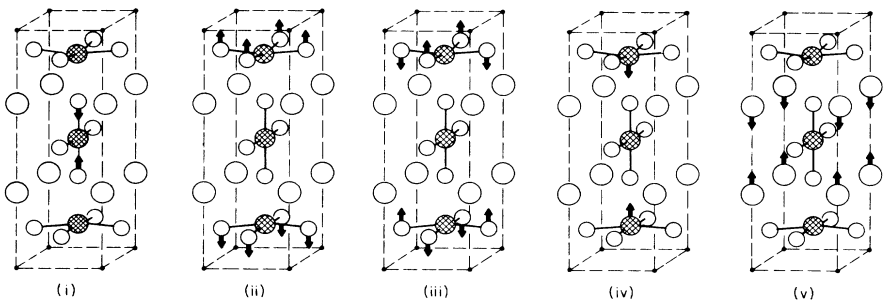

FIG. 2. The A_g vibrational modes (point group D_{2h}) of the $Ba_2YCu_3O_7$ structure. For tetragonal symmetry (point group D_{4h}), motions (i), (ii), (iv), and (v) are A_{1g} modes and (iii) is a B_{1g} mode. The atoms are the same as in Fig. 1 except for Y which has been omitted for simplicity.

TABLE I. Cu—O bond lengths and vibrational Raman frequencies (measured at room temperature). Bond lengths are taken from Refs. 20, 21, and 24.

	$Ba_2YCu_3O_6$ $a=3.857$, $c=11.819$	$Ba_2YCu_3O_7$ $a=3.820$, $b=3.885$, $c=11.676$	$Ba_{1.5}La_{1.5}Cu_3O_{7.25}$ $a=3.915$, $c=11.693$	$Sr_2YCu_{2.33}Al_{0.67}O_{7-\delta}$ $a=3.813$, $b=3.816$, $c=11.303$
Cu(1)—O(1)	1.795	1.846	1.851	1.707
Cu(2)—O(1)	2.469	2.295	2.199	2.258
Cu(2)—O(2)	1.941	1.930	1.969	1.923
Cu(2)—O(3)	1.941	1.961	1.969	1.923
Cu(1)—Cu(2)	4.264	4.141	4.050	3.965
(i)	475	505	535	545
(ii)	453	435	435	450
(iii)	335	335	288	335

Polarized Raman spectra on single crystals have been reported by only a few groups.[7–13] We focus on assignments made on the basis of single-crystal results here. Krol *et al.*[8] and Liu *et al.*[11] both assign the 500-, 435-, and 340-cm^{-1} features to the Cu-O stretching and bending modes (i), (ii), and (iii) above, respectively. Burns *et al.*[9] also agree with these assignments and attribute the 500-cm^{-1} feature to mode (i) and the 340-cm^{-1} feature to mode (iii). The Argonne group has emphasized the importance of these assignments in the interpretation of the isotope effect experiments (the effect on T_c of substituting ^{18}O for ^{16}O) and suggest that the 500-cm^{-1} mode is due to vibrations of O(2) and O(3) rather than O(1) (Refs. 10 and 23).

Several calculations of the lattice dynamics have found that the Cu(2) axial stretching mode should lie at higher frequency than the Ba mode.[2,11,18] This led Krol *et al.*[8] to assign these modes to the 220- and 140-cm^{-1} features, respectively. Liu *et al.*[11] and Hadjiev and Iliev[12] assign the Cu and Ba modes to the 140- and 116-cm^{-1} features, respectively, and ascribe the 220-cm^{-1} feature to defect-induced scattering. In a Raman study of electronic scattering processes, Cooper *et al.*[15] have observed strong interactions between the 340- and 116-cm^{-1} phonons and a broad electronic continuum feature. These authors assign the 340- and 116-cm^{-1} features to modes that involve the Cu(2) planes [modes (iii) and (iv) above] to explain the strong coupling to the electronic continuum and prefer that the Ba mode be associated with the 140-cm^{-1} feature; i.e., they reverse the order of the two low-frequency modes expected from lattice-dynamics calculations.

In the following we address the assignment of the O(1) axial stretching vibration [mode (i) above] and the Cu(2) vibration [mode (iv)].

A. The 500-cm^{-1} mode: Correlation with Cu—O(1) bond lengths

Raman spectra for ceramics of three materials with the triple perovskite structure are shown in Fig. 3. The features which have been assigned to oxygen vibrations are shown. [We note that the frequency of the 545-cm^{-1} feature shown for $Sr_2YCu_{2.3}Al_{0.7}O_7$ is the same for ceramic samples with Al contents of 0.4 and 0.9. Hence, it appears that the Al, which substitutes on the Cu(1) site and is not involved in the Raman active motions, does not strongly affect the frequency of the 545-cm^{-1} feature.] The frequencies of these oxygen-related features and the Cu—O bond lengths for the different materials are shown in Table I. We have labeled the frequencies by the mode assignments we favor and will provide additional support for these assignments below. Although not shown in Fig. 3, Raman spectra have been measured by several groups[2,5] for $Ba_2YCu_3O_6$ (which is also included in Table I) and also intermediate oxygen contents.[4,5,25,26]

For the materials shown in Table I, the Cu(1)—O(1) and Cu(2)—O(1) bond lengths change by as much as ~8% while the changes in the Cu(2)—O(2) and Cu(2)—O(3) bond lengths are smaller (only ~2%). From the $Ba_2YCu_3O_x$ structure it is expected that substi-

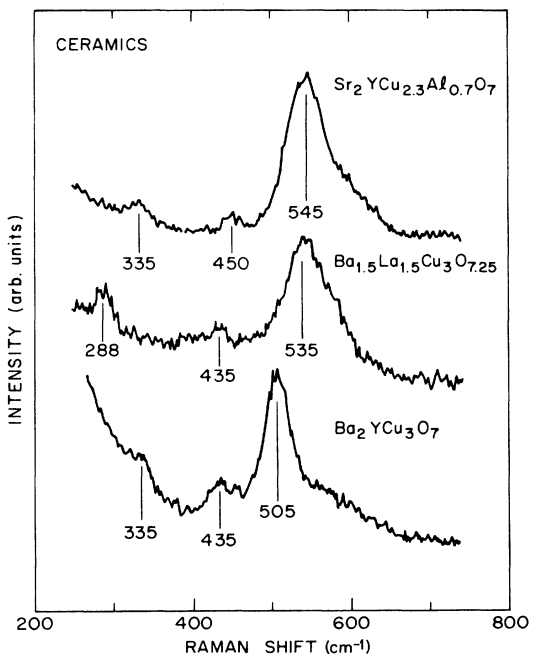

FIG. 3. Raman spectra of ceramics of three compounds with the triple perovskite structure.

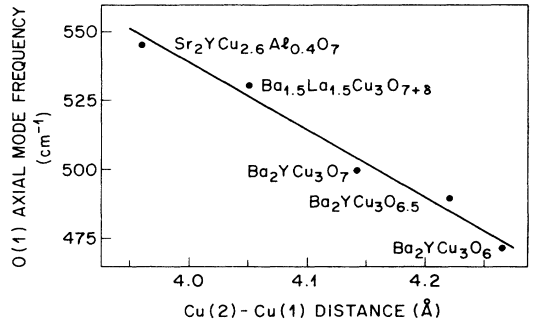

FIG. 4. The frequency of the O(1) axial breathing mode vs Cu(2)-Cu(1) distance for several compounds with the triple perovskite structure. (The point for $Ba_2YCu_3O_{6.5}$ was taken from Ref. 4.)

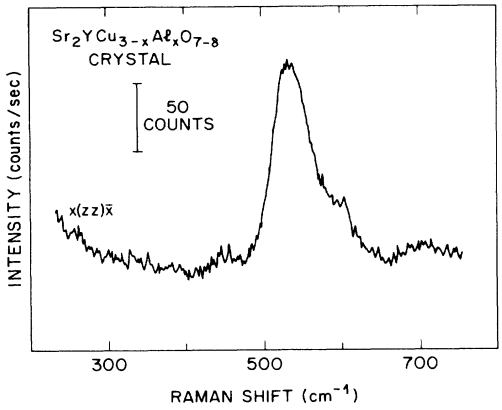

FIG. 5. Raman spectrum taken with $x(zz)\bar{x}$ polarization in a backscattering configuration from the thin crystal edge for $Sr_2YCu_{3-x}Al_xO_{7-\delta}$.

tutions on the alkaline earth site would have the greatest effect on the bond lengths along the c axis. Of the oxygen-related modes, the largest frequency changes for the different materials occur for mode (i). [Mode (i) shifts by 70 cm^{-1} while mode (ii) shifts by only < 20 cm^{-1}. As we have discussed earlier, mode (iii) is already definitively assigned.] We take these large frequency shifts for the $\sim$500-cm^{-1} feature upon changes of the Cu—O(1) bond lengths to be strong evidence that the 500-cm^{-1} feature is due to O(1) axial stretching.

From Table I it can be seen that neither the Cu(1)—O(1) nor the Cu(2)—O(1) bond length changes correlate well with the changes in the mode (i) frequency. However, the sum of these distances, i.e., the Cu(1)-Cu(2) distance correlates very well as we show in Fig. 4. We conclude that the Cu(1)—O(1) bond does not dominate the frequency of mode (i) despite its shorter bond length and that the Cu(2)-O(1) force constant must also be important.

B. Vibrational Raman scattering from $Sr_2YCu_{3-x}Al_xO_{7-\delta}$ single crystals

Raman spectra of $Sr_2YCu_{3-x}Al_xO_{7-\delta}$ single crystals for the different polarization geometries are shown in Figs. 5 and 6. These spectra are very similar to those obtained for $Ba_2YCu_3O_x$ and can be interpreted so as to strengthen the assignments of the modes in both compounds. We note that the $Sr_2YCu_{3-x}Al_xO_{7-\delta}$ crystals are either tetragonal for oxygen-deficient compositions or have a very small orthorhombic distortion for oxygen-annealed samples. We ignore the small orthorhombic distortion and present assignments in terms of the point group D_{4h}.

The spectrum for zz polarization taken with the Raman microscope is shown in Fig. 5. The strong band near 540 cm^{-1} only appears in the zz polarization geometry as was also the case for the 500 cm^{-1} band in $Ba_2YCu_3O_7$. As was described above, this band is assigned to the A_{1g} mode that involves axial, symmetric stretching of the O(1) atoms.

The band at 330 cm^{-1} in Figs. 6(a) and 6(b) has distinctive polarization selection rules. It is seen in the xx polarization geometry (x and y are along the crystallographic axes) and the $x'y'$ geometry (where the crystal has been rotated by 45° about the c axis). No other modes are seen in the $x'y'$ geometry. These selection rules are characteristic of a mode with B_{1g} symmetry. [For B_{1g} modes the polarizability tensor has the nonzero components $\alpha_{xx} = -\alpha_{yy}$ for the unrotated coordinates and hence only scattering for parallel polarizations. Rotation by 45° about c gives a polarizability tensor with the nonzero components $\alpha_{x'y'} = \alpha_{y'x'}$ for the rotated coordinates and hence only depolarized scattering. The A_{1g} modes have $\alpha_{xx} = \alpha_{yy}$ and hence no depolarized scattering

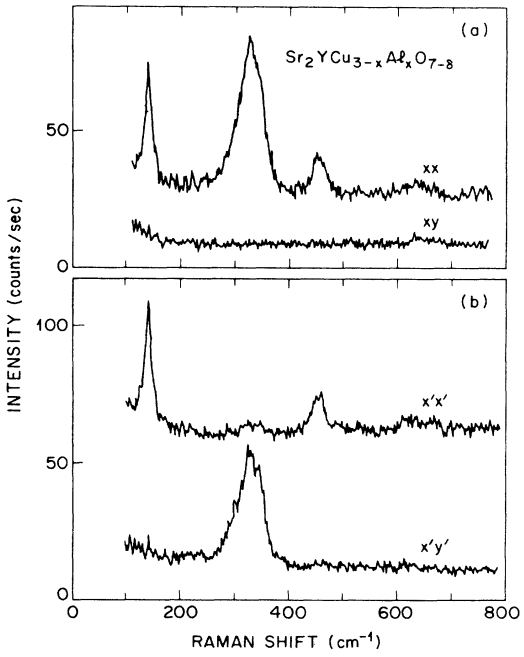

FIG. 6. Raman spectra taken in a 90° scattering geometry from the c face of a $Sr_2YCu_{3-x}Al_xO_{7-\delta}$ crystal. (a) The x and y axes are along the crystallographic axes. (b) The crystal has been rotated 45° about the c axis so that x' is 45° from the crystallographic a axis.

upon rotation of the crystal about c.] Only the Cu(2)–O(2) and Cu(2)–O(3) bond-bending mode in which O(2) and O(3) move out of phase, mode (iii) above, has the required B_{1g} symmetry and hence can be definitively assigned to the 330-cm^{-1} mode.

The remaining A_{1g} mode, Cu(2)–O(2) and Cu(2)–O(3) bond bending with O(2) and O(3) moving in phase, is assigned to the 450-cm^{-1} feature.

The low-frequency region of the spectrum for $Sr_2YCu_{3-x}Al_xO_{7-\delta}$ is compared to that of an oxygen-deficient $Ba_2YCu_3O_x$ crystal (annealed for 20 h in N_2 at 700 °C) in Fig. 7. For the $Ba_2YCu_3O_x$ crystal, Raman features are observed at 140 and 112 cm^{-1}. (The 112-cm^{-1} feature has been observed at 116 to 120 cm^{-1} by others.[9,10,12,13]) For the Sr compound only a band with A_{1g} symmetry at 140 cm^{-1} is seen.

In both materials we would expect mode (iv), axial breathing of the Cu(2) atoms, to have similar frequencies. Sr is much lighter than Ba so we would expect mode (v), axial breathing of the Ba atoms in $Ba_2YCu_3O_x$, to increase in frequency for the Sr compound. Our results therefore support the assignment of the 140 cm^{-1} band in $Ba_2YCu_3O_x$ to the Cu(2)-related mode because it is unshifted for the Sr compound. The 112-cm^{-1} mode is then assigned to the Ba mode. If we roughly estimate the upward shift of the Ba mode upon replacement by Sr by assuming the mode frequency is inversely proportional to the square root of the ratio of the Ba and Sr masses then this mode would be expected to lie near 140 cm^{-1}, coincident with the Cu(2) mode. Such a shift would explain the apparent disappearance of the 112-cm^{-1} mode and also the increased width of the 140-cm^{-1} band for the Sr compound.

In spite of the simplicity of the assignments of the 140- and 118-cm^{-1} features given above, they cannot be considered as definitive as the assignment of the B_{1g} feature made on the basis of polarization selection rules. The upward frequency shift of the weak 112-cm^{-1} feature upon the substitution of Sr for Ba is not actually observed; its possible coincidence with the 140-cm^{-1} band is speculative. Further, there is no simple explanation for the strong coupling of the 112-cm^{-1} feature to the electronic continuum[15] in the context of its assignment to the Ba mode. However, with these reservations noted, our data on Ba substitution by Sr and the lattice dynamics calculations[2,11,18] lead us to favor the assignment of the 140-cm^{-1} feature to the Cu mode and the 112-cm^{-1} feature to the Ba mode.

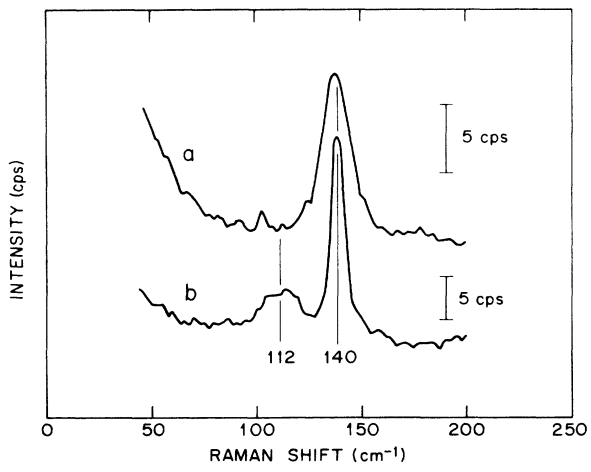

FIG. 7. Raman spectra taken for xx polarization in a 90° scattering geometry for single crystals of (a) $Sr_2YCu_{3-x}Al_xO_{7-\delta}$ and (b) $Ba_2YCu_3O_x$ (N_2 annealed).

Finally, we remark that the features near 600 and 220 cm^{-1} that were observed for $Ba_2YCu_3O_x$ are relatively weaker or absent in the Sr compound. These features are attributed to defect-induced scattering. There is much less variability in the oxygen content in the $Sr_2YCu_{3-x}Al_xO_{7-\delta}$ than for $Ba_2YCu_3O_x$; hence we might expect scattering related to oxygen vacancy disorder to be less prominent in these materials. The broad feature near 600 cm^{-1} is ~30 cm^{-1} higher in frequency for the Sr compound (see Fig. 6) than for $Ba_2YCu_3O_x$. The higher frequency for planar and chain Cu-O stretching that are allowed by disorder is consistent with the shorter planar bond lengths (see Table I) for the Sr compound.

IV. CONCLUSION

We have examined the Raman spectra of triple perovskites with the $Ba_2YCu_3O_x$ structure that have been substituted on the Ba site to gain additional evidence to support the phonon assignments. Large changes in the Cu(2)-O(1) and Cu(1)-O(1) distances upon substitution and the consequent large changes in the ~500-cm^{-1} feature's frequency, provide additional support for the assignment of the ~500-cm^{-1} feature to O(1) axial stretching. The definitive assignment on the basis of polarization selection rules of the 330–340-cm^{-1} feature in $Ba_2YCu_3O_x$ and $Sr_2YCu_{3-x}Al_xO_{7-\delta}$ to the B_{1g} mode that involves Cu(2)–O(2) and Cu(2)–O(3) bond-bending with the O(2) and O(3) moving out of phase leaves the 435–450-cm^{-1} feature to be assigned to Cu(2)–O(2) and Cu(2)–O(3) bond bending with O(2) and O(3) moving in phase. These assignments of the Cu-O modes are in agreement with the expectations of lattice-dynamics calculations and also account for the relative sizes for the elements of the polarizability tensor as was discussed in Refs. 8, 9, 11, and 12.

The presence of the 140-cm^{-1} band in both $Ba_2YCu_3O_x$ and $Sr_2YCu_{3-x}Al_xO_{7-\delta}$ supports the assignment of this feature to the axial breathing motion of the Cu(2) atoms. The ~112-cm^{-1} feature in $Ba_2YCu_3O_x$ is then assigned to the axial breathing of the Ba atoms. Having the Ba mode lie below the Cu(2) mode is in agreement with several lattice dynamics calculations[2,11,18] but does not provide a simple explanation for why this Ba mode couples strongly to the conduction electrons as was observed by Cooper *et al.*[15]

ACKNOWLEDGMENTS

We thank T. Siegrist for numerous conversations on the structure and composition of the materials examined here.

[1]H. Rosen, E. M. Engler, T. C. Strand, V. Y. Lee, and D. Bethune, Phys. Rev. B **36**, 726 (1987); R. M. Macfarlane, H. Rosen, and H. Seki, Solid State Commun. **63**, 831 (1987).

[2]M. Stavola, D. M. Krol, W. Weber, S. A. Sunshine, A. Jayaraman, G. A. Kourouklis, R. J. Cava, and E. A. Rietman, Phys. Rev. B **36**, 850 (1987).

[3]L. Ran, R. Merlin, M. Cardona, Hj. Mattausch, W. Bauhofer, and A. Simon, Solid State Commun. **63**, 839 (1987).

[4]G. A. Kourouklis, A. Jayaraman, B. Batlogg, R. J. Cava, M. Stavola, D. M. Krol, E. A. Rietman, and L. F. Schneemeyer, Phys. Rev. B **36**, 8320 (1987).

[5]A. Wittlin, R. Liu, M. Cardona, L. Genzel, W. König, W. Bauhofer, Hj. Mattausch, and A. Simon, Solid State Commun. **64**, 477 (1987); C. Thomsen, R. Liu, M. Bauer, A. Wittlin, L. Genzel, M. Cardona, E. Schönherr, W. Bauhofer, and W. König, *ibid.* **65**, 55 (1988).

[6]A more complete set of references to the many Raman studies on $Ba_2YCu_3O_x$ is contained in G. Burns, F. H. Dacol, P. P. Freitas, W. König, and T. S. Plaskett, Phys. Rev. B **37**, 5171 (1988).

[7]R. J. Hemley and H. K. Mao, Phys. Rev. Lett. **58**, 2340 (1987).

[8]D. M. Krol, M. Stavola, W. Weber, L. F. Schneemeyer, J. V. Waszczak, S. M. Zahurak, and S. G. Kosinski, Phys. Rev. B **36**, 8325 (1987).

[9]G. Burns, F. H. Dacol, F. Holtzberg, and D. L. Kaiser, Solid State Commun. **66**, 217 (1988).

[10]R. Bhadra, T. O. Brun, M. A. Beno, B. Dabrowski, D. G. Hinks, J. Z. Liu, J. D. Jorgensen, L. J. Nowicki, A. P. Paulikas, I. K. Schuller, C. U. Segre, L. Soderholm, B. Veal, H. H. Wang, J. M. Williams, K. Zhang, and M. Grimsditch, Phys. Rev. B **37**, 5142 (1988).

[11]R. Liu, C. Thomsen, W. Kress, M. Cardona, B. Gegenheimer, F. W. deWette, J. Prade, A. D. Kulkarni, and U. Schröder, Phys. Rev. B **37**, 7971 (1988).

[12]V. G. Hadjiev and M. N. Iliev, Solid State Commun. **66**, 451 (1988).

[13]C. Thomsen, M. Cardona, B. Gegenheimer, R. Liu, and A. Simon, Phys. Rev. B **37**, 9860 (1988).

[14]J. C. Phillips, Phys. Rev. Lett. **59**, 1856 (1987).

[15]S. L. Cooper, M. V. Klein, B. G. Pazol, J. P. Rice, and D. M. Ginsberg, Phys. Rev. B **37**, 5920 (1988).

[16]J. D. Jorgensen, in *Proceedings of the Eighteenth International Conference on Low Temperature Physics, Kyoto, 1987* [Jpn. J. Appl. Phys. **26**, Suppl. 26-3, 2017 (1987)].

[17]T. Siegrist, S. A. Sunshine, D. W. Murphy, R. J. Cava, and S. M. Zahurak, Phys. Rev. B **35**, 7137 (1987).

[18]F. E. Bates and J. E. Eldridge, Solid State Commun. **64**, 1435 (1987).

[19]D. B. Mitzi, A. F. Marshall, J. Z. Sun, D. J. Webb, M. R. Beasley, T. H. Geballe, and A. Kapitulnik (unpublished).

[20]S. A. Sunshine, L. F. Schneemeyer, J. V. Waszczak, D. W. Murphy, S. Miraglia, A. Santoro, and F. Beech, J. Cryst. Growth **85**, 632 (1987).

[21]L. F. Schneemeyer, S. A. Sunshine, R. B. van Dover, E. M. Gyorgy, J. V. Waszczak, and T. Siegrist (unpublished).

[22]A preliminary report of this work appears in D. M. Krol, M. Stavola, L. F. Schneemeyer, J. V. Waszczak, and W. Weber, in *High Temperature Superconductors,* edited by M. B. Brodsky, R. C. Dynes, K. Kitazawa, and H. L. Tuller, Materials Research Symposia Proceedings, Vol. 99 (Materials Research Society, Pittsburgh, 1988), p. 781.

[23]M. Grimsditch *et al.*, Phys. Rev. Lett. **60**, 752 (1988); B. Batlogg, R. J. Cava, and M. Stavola, *ibid.* **60**, 754 (1988).

[24]A. Santoro, S. Miraglia, F. Beech, S. A. Sunshine, D. W. Murphy, L. F. Schneemeyer, and J. V. Waszczak, Mater. Res. Bull. **22**, 1007 (1987); S. Miraglia, F. Beech, A. Santoro, D. Tran Qui, S. A. Sunshine, and D. W. Murphy, *ibid.* **22**, 1733 (1987).

[25]R. M. Macfarlane, H. J. Rosen, E. M. Engler, R. D. Jacowitz, and V. Y. Lee, Phys. Rev. B **38**, 284 (1988).

[26]M. Hangyo, S. Nakashima, K. Mizoguchi, A. Fujii, A. Mitsuishi, and T. Yotsuya, Solid State Commun. **65**, 835 (1988).